Highlighting research from Tokyo Tech from the group of Prof. Atsushi Shishido.

Thermo-, photo-, and mechano-responsive liquid crystal networks enable tunable photonic crystals

Multi-stimuli responsive photonic crystals enable one to develop novel mechanical and optical devices such as soft sensors and actuators. Akamatsu *et al.* successfully designed bendable liquid crystal photonic crystals which respond to thermo-, photo- and mechano-stimuli.

ROYAL SOCIETY
OF CHEMISTRY

rsc.li/soft-matter-journal

Soft Matter

PAPER

Thermo-, photo-, and mechano-responsive liquid crystal networks enable tunable photonic crystals†

N. Akamatsu,[a] K. Hisano, [ID][a] R. Tatsumi,[a] M. Aizawa,[a] C. J. Barrett [ID][ab] and A. Shishido [ID] *[ac]

Tunable photonic crystals exhibiting optical properties that respond reversibly to external stimuli have been developed using liquid crystal networks (LCNs) and liquid crystal elastomers (LCEs). These tunable photonic crystals possess an inverse opal structure and are photo-responsive, but circumvent the usual requirement to contain dye molecules in the structure that often limit their applicability and cause optical degradation. Herein, we report tunable photonic crystal films that reversibly tune the reflection peak wavelength under thermo-, photo- and mechano-stimuli, through bilayering a stimuli-responsive LCN including azobenzene units with a colourless inverse opal film composed of non-responsive, flexible durable polymers. By mechanically deforming the azobenzene containing LCN via various stimuli, the reflection peak wavelength from the bilayered film assembly could be shifted on demand. We confirm that the reflection peak shift occurs due to the deformation of the stimuli-responsive layer propagating towards and into the inverse opal layer to change its shape in response, and this shift behaviour is repeatable without optical degradation.

Introduction

Photonic crystals that exhibit periodic refractive-index structure at the nanoscale level ranging from one to three dimensions possess unique transmission, reflection, diffraction and refraction properties by controlling light propagation at wavelengths corresponding to the periodicity. This unique property could enable researchers to develop applications in various advanced photonic devices, such as optical waveguides, low-threshold lasers and optical switches.[1,2] Although such photonic crystals have been traditionally designed via semiconductor processing in a 'top-down' manner, these usual fabrication methods often require significant cost and time for microfabrication, and suffer constraints on processing the size that render them unfavourable for producing photonic crystals that could be applied to short visible (Vis) and ultraviolet (UV) wavelengths of light.[3–5] Recently, as a facile alternate method of fabricating photonic crystals, self-assembly in a 'bottom-up' manner has attracted much attention. These methods could possess great

advantages in material design capabilities over top-down processes and are relatively simple and inexpensive in fabrication, thus enabling the fabrication of smaller-period photonic crystals that are responsive in the UV-Vis regions.[6,7] A representative example of such bottom-up fabrication is an opal structure with a three-dimensional periodic arrangement via self-assembly of monodispersed nano-particles. The voids in opal structure could then be back-filled with a soft flexible polymer material, and further the template opal structure could be removed to create an inverse opal structure while maintaining the initial periodicity and associated optical properties. These inverse opal structures exhibit high dynamic strength compared with the initial opal structure composed of nano-particles. Thus, the periodic structure could be resilient and robust to external stresses such as bending, friction or impact. Recently, the mechanical stability of such soft inverse opal photonic crystals and their periodicity-defined optical properties have been shown to be tunable, *i.e.*, changing their structure and thus their optical characteristics in response to external fields such as stress, light and heat. Such dynamic photonic materials with optical properties varying under external fields, *i.e.*, tunable photonic crystals, are promising materials for applications in a wide range of technologies, including next generation dynamic displays, rapid-response environmental sensors and wearable 'smart' devices.[8–12]

The preparation of gels from a wide variety of material systems has been continuously studied for the development

[a] *Laboratory for Chemistry and Life Science, Institute of Innovative Research, Tokyo Institute of Technology, 4259 Nagatsuta, Midori-ku, Yokohama 226-8503, Japan. E-mail: ashishid@res.titech.ac.jp; Tel: +81-45-924-5242*

[b] *Department of Chemistry, McGill University, Montreal, Quebec, Canada*

[c] *Precursory Research for Embryonic Science and Technology (PRESTO), Japan Science and Technology Agency (JST), 4-1-8 Honcho, Kawaguchi 332-0012, Japan*

† Electronic supplementary information (ESI) available. See DOI: 10.1039/c7sm01287j

of tunable photonic crystals. The swelling ratio of gels with an inverse opal structure varies according to the temperature or the pH of the solvent and exposure to chemical species. Consequently, such external environmentally-induced expansion or contraction of the period of the structure leads to a clear shift in the peak wavelength of the reflected light derived from the structure.[13–16] Specifically, Asher *et al.* succeeded in producing an inverse opal gel containing an azobenzene photochromic compound, and provided the development of the first generation of photo-responsive photonic crystals.[17] The swelling ratio of these gel-containing azobenzene materials to the solvent exhibits a significant dependence on the polarity, tuned *via* the *trans–cis* geometric photo-isomerization. The azo isomerization by light irradiation leads to repeated swelling-de-swelling of the gel. Consequently, the distance between the particles changes, and the reflection peak wavelength shifts reversibly by approximately 60 nm. Takeoka *et al.* also developed a multi-tunable photonic crystal that is responsive to light and thermal stimuli by creating an inverse opal gel composed of both azobenzene and poly-(*N*-isopropyl) acrylamide.[18] However, as observed in most of these previous studies, application of tunable photonic crystals to various types of optical devices such as optical filters and displays, has been reported to be difficult because of the necessity of using water or an organic solvent as well as complicated handling requirements and restrictions on environment. The range of applications of tunable photonic crystals would expand significantly if the reversible peak shift of reflected light could be achieved in a dry system that does not require the use of a solvent, which remains a key goal towards the development of dynamic responsive photonic crystals.

Liquid crystal networks (LCNs) and liquid crystal elastomers (LCEs) are attractive materials towards achieving this aim because they could undergo reversible expansion or contraction in dry environments.[19–22] The molecular orientation in LCNs and LCEs could respond to various external stimuli, such as stress, heat, light and changes in intermolecular distance. Such responses could be controlled in regions where contraction occurs with stimulation along the orientation direction, and the expansion results with perpendicular stimulus.[23–25] Such careful spatial design of the molecular orientation direction could provide reversibly-induced arbitrary deformation behaviour. Thus, several studies have focused on the use of stimuli-responsive materials in dry systems for two-dimensional and three-dimensional shape control. This feature has been used by various studies to demonstrate that the wavelength of reflected light in LCEs or LCNs, possessing an inverse opal structure, could shift predictably in response to stress,[26] heat[27–29] or light.[30,31] Moreover, dual-responsive photonic crystals have been fabricated using a solvent-free process.[32,33] However, in a conventional material system, the inverse opal structure could gradually become disordered when the shape deforms repeatedly, deteriorating the desired optical characteristics. To solve this problem, the material we developed and present herein decouples the function of the stimuli-responsive deformation behaviour and that of the photonic crystal to impart improved stability to the periodic optical structure in a completely dry environment.

A photo-responsive LCN film was successfully produced using azobenzene,[34,35] and combined with a flexible inverse opal film, to create a material with a periodic structure that is stable to repeated bending.[36,37] The results also indicate (for the first time) that the composite films obtained on bilayering the two films correspond to multi-responsive tunable photonic crystals. Herein, we report a proof-of-principle demonstration that the bilayer tunable photonic crystal fabricated in this study responds to various stimuli, including light, heat and mechanical stress, and that it is thus possible to reversibly control the reflection peak wavelength. The periodic structure of this inverse opal film changes with respect to the timescale of deformation; thus, the reflection peak wavelength shifts rapidly. However, the structure of the flexible inverse opal film is robust and it could respond to repeated stimuli without deterioration of the desired optical characteristics.

Results and discussion

A bilayered film comprising a flexible inverse opal film (**IO**) and a photo-responsive azo LCN (**Az**), in which azobenzene is uniaxially oriented (an **IO/Az** film), was prepared based on the synthetic procedures of similar compounds described previously.[36,37] This was followed by film production and an evaluation of the resultant inverse opal structure (Fig. 1). The thickness of the obtained film was 105 μm, including the 20 μm photo-responsive layer. Differential scanning calorimetry (DSC) thermograms for each layer of the stimuli-responsive bilayered film (Fig. S1, ESI†) reveal the glass transition temperatures (T_g) to be around 20 °C. The wavelength (λ) of the light Bragg-reflected by the inverse opal structure depends on the incident angle, thickness, and refractive index (eqn (1)) and thus a detailed treatment is required.

$$\lambda_{max} = 2\sqrt{\frac{2}{3}}d\sqrt{\sum_i n_i^2 \phi_i - \sin^2\theta} \qquad (1)$$

where λ_{max} denotes the reflection peak wavelength, d denotes pore diameter, n denotes the refractive index of each component,
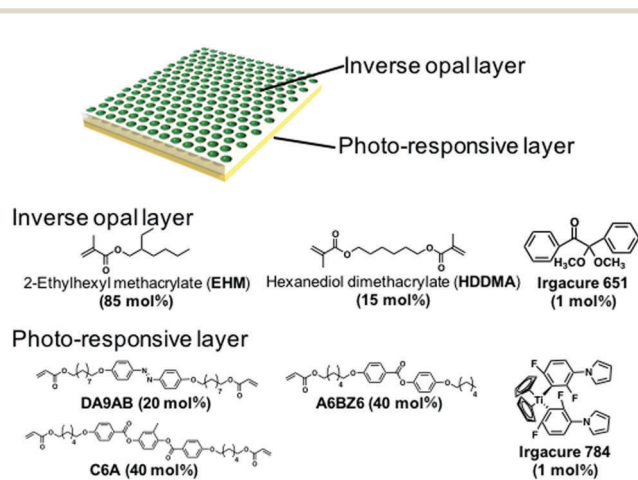

Fig. 1 A schematic illustration of bilayered film and the chemical structures of materials used for the fabrication of inverse opal film (top layer) and of photo-responsive film (bottom layer).

ϕ denotes the volume fraction of each component and θ denotes the incident angle of light.

First, we evaluated the incident-angle dependence of a reflection peak. The measured values were compared with the expected Bragg reflection wavelength estimated using the theoretical formula of eqn (1) by placing the detector at different positions and using the light source, which is, Fibre-guided light (FLH-50, manufactured by Shimadzu Corporation). When the incident angle increased, the reflection peak wavelength was blue-shifted; the incident-angle dependence of the peak wavelength of **IO/Az** films is illustrated in Fig. 2a. The angle dependence of the theoretical reflection wavelength corresponds to a value calculated using the pore diameter of 299 nm in the inverse opal film as demonstrated from a previous study and eqn (1). The observed reflection peak wavelength was in good agreement with the calculated value for each incident angle. This suggests that the inverse opal film exhibits an array of face-centred cubic structures with little disturbance.

Next, the light source and the reflection probe (detector) were installed at the same position, and the incident-angle dependence was again examined as described earlier (Fig. 2b). An increase in the incident angle decreased the reflectance and led to a shift in the reflection peak wavelength. The reflectance for incident angles exceeding 10° was reduced below the limit of detection. The shift in the reflection peak wavelength was within several nanometres for incident angles below 10°. This means that the incident angle presumably does not affect the reflection peak shift. Thus, we employed the optical setup as shown in Fig. 2b for measuring reflection properties of **IO/Az** films under various stimuli.

Furthermore, the behaviour of an **IO/Az** film under various deformations caused by thermal-stimulus was investigated for the effect on the reflection peak wavelength. The reflection spectra were measured with the **IO/Az** film sandwiched between glass substrates on a hot stage; the reflection peak wavelength at each temperature is shown in Fig. 3a. The reflection peak wavelength was observed to be 555 nm at room temperature and was red-shifted to 567 nm after heating at 160 °C. On cooling to room temperature, the reflection peak wavelength blue-shifted back to 555 nm; thus, the results indicate that the shift in the reflection peak due to the changes in temperature was completely reversible. Furthermore, this reversible peak shift could be repeatedly induced (Fig. 3b). The uniaxial orientation of the **Az** layer is observed to be disordered under thermal stimulus, and contraction in this layer occurs typically along the alignment direction. Therefore, we propose that the inverse opal layer is compressed in the alignment direction and expanded in the film-thickness direction, and that this phenomenon is responsible for the red-shift of the reflection peak. In addition, it is expected that the inverse opal layer thermally expands and the distance between pore centres increase, contributing to the wavelength shift. As already mentioned, previous studies have reported that the reflection peak wavelength blue-shifts by as much as 120 nm due to a phase transition caused by heating the LCN with an inverse opal structure.[27] However, the change in the peak wavelength was irreversible in this case because the periodicity of the opal structure collapsed during the phase transition. Conversely, in the **IO/Az** film used herein, although the peak-shift width was as small as 12 nm, it exhibited a high potential for application as a thermo-responsive tunable photonic crystal since the wavelength shift in this film could be stable and repeatedly induced.
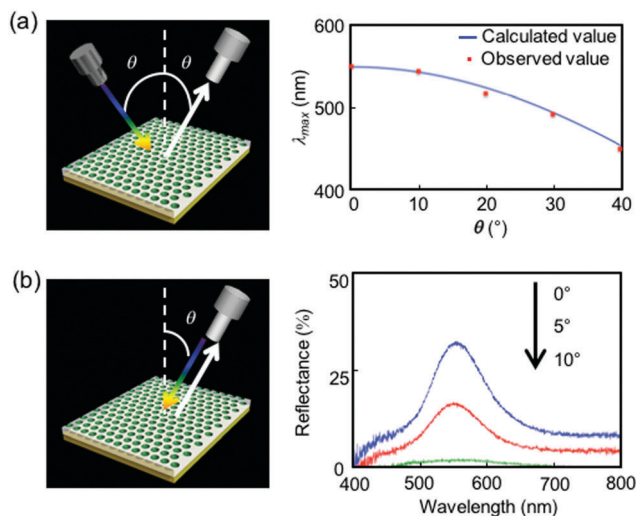

Fig. 2 (a and b) Optical setups for reflection spectra measurement using fiber-guided light with a detector at the symmetric and the reflection probe (detector), respectively (left). (a, right) Reflection-peak wavelength of the bilayered film as a function of the angle of incident light. (b, right) Reflection spectra of the bilayered film using incident light set at 0, 5 or 10°.
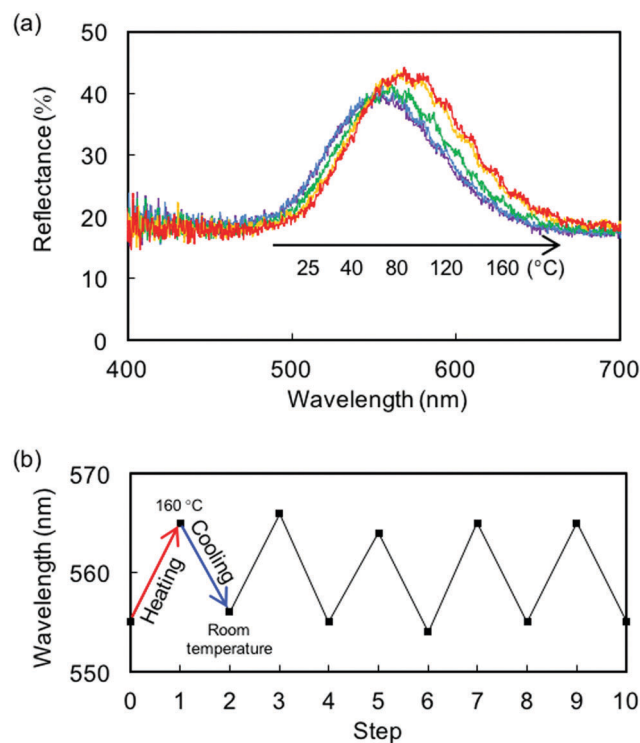

Fig. 3 (a) Reflection spectra of bilayered film as a function of wavelength by thermal heating at 25, 40, 80, 120 or 160 °C. (b) Reflection peak wavelength of bilayered film under reversibly heating and cooling cycles.

The photo-induced bending behaviour of the **IO/Az** film was then investigated, and the results are presented in Fig. 4. We irradiated the fabricated film using either UV light (UV-LED: UV-400, manufactured by Keyence Corporation) with a wavelength of 365 nm and light intensity of 100 mW cm^{-2} or Vis light (Vis-LED; PJ-150-2 CA, HLV-24 GR-NR-3 W, manufactured by CCS) with a wavelength of 530 nm and light intensity of 30 mW cm^{-2}. When the film was irradiated with UV light through the inverse opal layer, it reached maximum bending towards the **Az**-layer side along the direction of the mesogen orientation in approximately 70 s. Moreover, the film resumed its original shape in approximately 70 s under irradiation with Vis light. Even when the film was irradiated with UV light from the **Az**-layer side under the same conditions, the film reached a maximum bending in the direction of the mesogen orientation towards the **Az**-layer side in approximately 60 s. The film resumed its original shape in approximately 70 s under irradiation with Vis light. Following irradiation with UV light, contraction due to photo-isomerization occurs in the **Az** layer. However, the inverse opal layer is not photo-responsive and does not change shape directly with light. Therefore, when irradiation is continued, the entire **Az** layer is photo-isomerized and only the **Az** layer shrinks anisotropically along the orientation direction. As a result, the bilayered film is considered to be bent towards the **Az**-layer side. In our obtained results, various films were produced by bilayering azobenzene LCN and polymer films, and we previously reported that when these systems are irradiated with UV light, the bilayered film always experiences bending towards the **Az**-layer side, irrespective of the direction of incidence.[38] This directional control has been employed previously with good success to induce complex deformations, such as sample rotational 'rolling', translational 'walking' motions, and robot-arm-like 'elbow' movements.[34,39] Therefore, it is expected that the photo-induced bending mechanism of the photo-responsive bilayered polymer films herein would also function similar to these previously reported bilayered structures.

To analyse the photo-responsiveness of the **IO/Az** films, the shift in the reflection peak wavelength due to photo-induced bending was examined using the optical setup shown in Fig. 2b. The film was irradiated with a UV-LED with a wavelength of 365 nm and light intensity of 100 mW cm^{-2} from the **Az**-layer side, as the reflection peak wavelength of the bending process was measured. Although the distance between the film surface and the reflection probe changed as the film bent, the change in distance only affected the reflection intensity, keeping the reflection peak wavelength constant. The angle supplementary to that formed by the tangents of the edges of the bent film is defined as the bending angle ϕ as depicted in the inset of Fig. 5a. A reflection peak appeared at a wavelength of 555 nm prior to irradiation with UV light. However, following UV irradiation, the reflection peak wavelength gradually blue-shifted as the bending angle increased, and it reached a wavelength of 539 nm via a blue-shift of 16 nm at the maximum bending angle (Fig. 5a). Furthermore, when the film was irradiated using a Vis-LED at a wavelength of 530 nm and light intensity of 30 mW cm^{-2}, the reflection peak wavelength red-shifted to 555 nm, thus resuming its original shape and initial state. Reversibility was confirmed by cycling repeatedly (Fig. 5b). The blue-shift of the peak shows a decrease in the period (*i.e.*, the periodic structure contracts); thus, the shrinkage factor at each bending angle was calculated using eqn (2) as follows:

$$\frac{d_2 - d_1}{d_1} \times 100 \tag{2}$$

Specifically, d_1 and d_2 denote pore diameters that are calculated before and after the peak shift from wavelengths λ_1 and λ_2, respectively, using eqn (1). The period decreased as the bending angle increased, and it is clear that the contraction ratio corresponded to 3.3% when the maximum bending was applied.

Fig. 5 (a and b) Reflection peak wavelength of bilayer film as a function of photo-induced bending angle (ϕ) of the film and under reversible UV and visible light irradiation cycles over time, respectively.
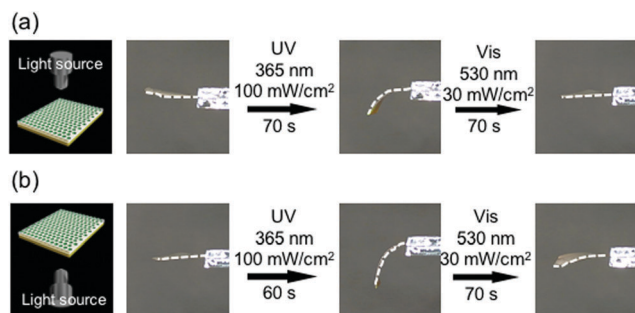

Fig. 4 (a and b) Photo-irradiation of a bilayered film from above (top) and below (bottom), respectively. Schematic illustration of the light irradiation setup and the appearance of film initially (left), under UV light irradiation (centre) and under visible light irradiation (right).
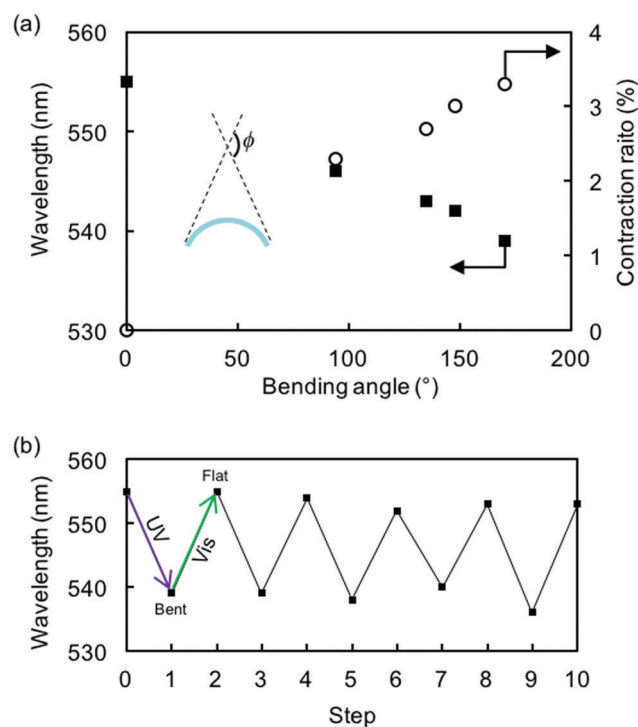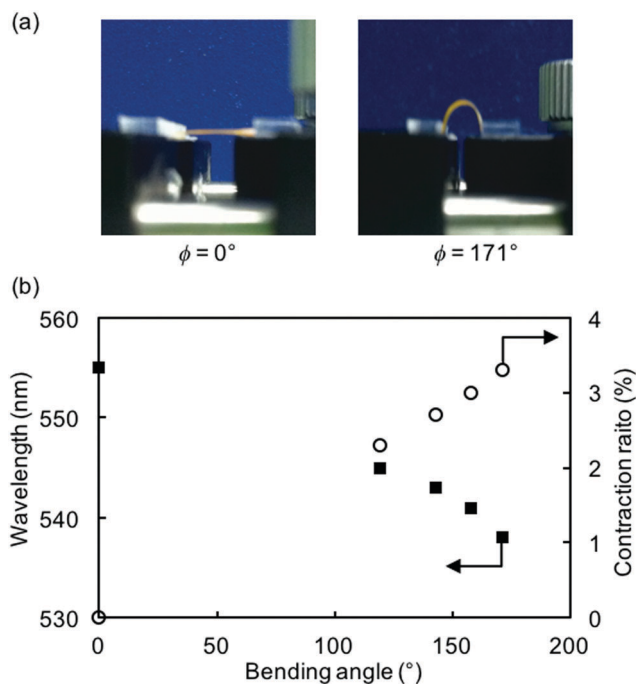
Fig. 6 (a) Photographs during mechanical bending of the bilayered film at bending angle of 0 and 171° (left, right). (b) Reflection-peak wavelength of the bilayered film observed as a function of mechanically-induced bending angle of the film.

Fig. 7 Schematic illustrations of shrinkage of inverse opal structures in the film-thickness direction at the surface of bilayered films when bent.

The shrinkage of this periodic structure could be rationalized quantitatively by the photo-induced bending behaviour of the photo-responsive bilayered polymer film. First, the **Az** layer contracted due to photo-irradiation; this was followed by bending of the **IO/Az** film. Subsequently, the inverse opal layer on the surface stretched because of this bending and thereby contracted towards the film-thickness direction. Tsutsui *et al.* produced an inverse opal structure using poly(methyl methacrylate) and reported that the pores underwent contraction in the film-thickness direction *via* thermal expansion. They further reported that the peak wavelength underwent a blue-shift when the period decreased.[26] Therefore, we expect that the periodic structure of the **IO/Az** film would shrink, and the reflection peak wavelength would exhibit a blue-shift similar to the results reported by Tsutsui *et al.* In contrast to previous reports, where the reflection of the film was coloured because photo-responsiveness was assigned to the inverse opal structure,[30–33] this study is the first example of the successful fabrication of a photo-responsive tunable photonic crystal that is colourless and reversibly photo-responsive.

If the inverse opal layer is stretched by bending of the **IO/Az** film, it is expected that the reflection peak wavelength would exhibit a similar blue-shift even when the film is mechanically bent. This was confirmed by attaching the **IO/Az** film to a sample holder and measuring the reflection spectrum at the time of bending caused by external stress (Fig. 6). The reflection peak wavelength prior to the bending corresponded to 555 nm. The peak wavelength blue-shifted with an increase in the bending angle. When the bending angle reached 169°, which
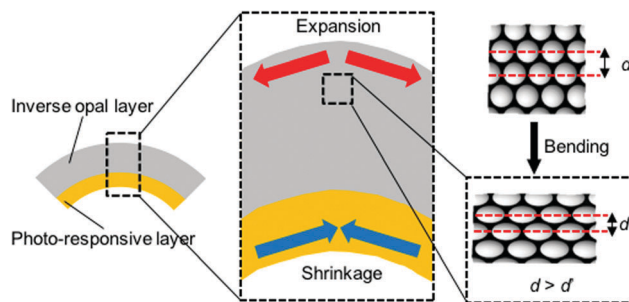
is approximately the same as the maximum bending angle obtained upon photo-induced deformation, the peak wavelength corresponded to 538 nm with a maximum blue-shift of 17 nm. The reflection peak wavelength also recovered to 555 nm when the film reverted back to the initial state. When the contraction ratio at each bending angle was calculated *via* eqn (2), using the same method as that described above, the contraction ratio corresponded to 3.3% at a bending angle of 171°. The measured results were in agreement with those obtained in the case of photo-induced deformation. Consequently, these results suggest that the reflection peak shift accompanying the photo-induced deformation of the **IO/Az** film was due to the surface stress resulting from bending. Generally, when a film is bent, the inside is compressed and the outside is stretched, separated by a neutral plane as a boundary that neither expands nor contracts at the time of bending (Fig. 7). The inverse opal layer was also stretched while bending the **IO/Az** film; thus, it is considered that the periodic structure of the surface shrank in the film-thickness direction, resulting in the blue-shift.

Conclusions

Bilayered films with a photo-responsive layer and a layer with photonic crystal properties were prepared, and their thermo-, photo-, and mechano-responsiveness were investigated. An **IO/Az** film with a free-standing inverse opal structure reversibly exhibited a 12 nm red-shift due to thermal expansion normal to the film surface when it was heated to 160 °C. This shift was reversibly restored repeatedly to its original reflection peak wavelength *via* cooling. Furthermore, the reflection peak wavelength exhibited a 16 nm blue-shift accompanying the photo-induced deformation caused by irradiation with UV light. This shift was also reversibly and repeatedly restored to the original reflection peak wavelength *via* irradiation with Vis light. The shift width depends on the bending angle, and identical results could be obtained even under bending caused by external mechanical stress. The results confirmed that the **IO/Az** film functions as a multi-tunable photonic crystal in which the reflection peak wavelength shifts to both sides of the longer and shorter wavelengths when stimulated with heat, light, or stress. The **IO/Az** film is the first example of a multi-tunable photonic crystal film obtained by bilayering the two films.

Since the inverse opal layer film itself is inherently colourless, it is potentially valuable for a variety of transparency-demanding photonic devices, such as optical filters and next-generation displays.

Conflicts of interest

There are no conflicts to declare.

Acknowledgements

Notes and references

1 E. Yablonovitch, *Phys. Rev. Lett.*, 1987, **58**, 2059.
2 S. John, *Phys. Rev. Lett.*, 1987, **58**, 2486.
3 S. Noda, A. Chutinan and M. Imada, *Nature*, 2000, **407**, 608.
4 A. Chutinan and S. Noda, *Appl. Phys. Lett.*, 1999, **75**, 3739.
5 M. Fujita, S. Takahashi, Y. Tanaka, T. Asano and S. Noda, *Science*, 2005, **308**, 1296.
6 S. H. Im, M. H. Kim and O. O. Park, *Chem. Mater.*, 2003, **15**, 1797.
7 Z. Z. Gu, A. Fujishima and O. Sato, *Chem. Mater.*, 2002, **14**, 760.
8 N. Akamatsu, W. Tashiro, K. Saito, J.-I. Mamiya, M. Kinoshita, T. Ikeda, J. Takeya, S. Fujikawa, A. Priimagi and A. Shishido, *Sci. Rep.*, 2014, **4**, 5377.
9 M. A. C. Stuart, W. T. Huck, J. Genzer, M. Müller, C. Ober, M. Stamm, G. B. Sukhorukov, I. Szleifer, V. V. Tsukruk, M. Urban, F. Winnik, S. Zauscher, I. Luzinov and S. Minko, *Nat. Mater.*, 2010, **9**, 101.
10 D. Ge, E. Lee, L. Yang, Y. Cho, M. Li, D. S. Gianola and S. Yang, *Adv. Mater.*, 2015, **27**, 2489.
11 H. Koerner, T. J. White, N. V. Tabiryan, T. J. Bunning and R. A. Vaia, *Mater. Today*, 2008, **11**, 34.
12 A. Shishido, *Polym. J.*, 2010, **42**, 525.
13 J. M. Weissman, H. B. Sunkara, A. S. Tse and S. A. Asher, *Science*, 1996, **274**, 959.
14 K. Lee and S. A. Asher, *J. Am. Chem. Soc.*, 2000, **122**, 9534.
15 H. Fudouzi and Y. Xia, *Langmuir*, 2003, **19**, 9653.
16 J. Ge, J. Goebl, L. He, Z. Lu and Y. Yin, *Adv. Mater.*, 2009, **21**, 4259.
17 M. Kamenjicki, I. K. Lednev, A. Mikhonin, R. Kesavamoorthy and S. A. Asher, *Adv. Funct. Mater.*, 2003, **13**, 774.
18 K. Matsubara, M. Watanabe and Y. Takeoka, *Angew. Chem., Int. Ed.*, 2007, **46**, 1688.
19 H. Finkelmann, E. Nishikawa, G. G. Pereira and M. Warner, *Phys. Rev. Lett.*, 2001, **87**, 015501.
20 T. J. White and D. J. Broer, *Nat. Mater.*, 2015, **14**, 1087.
21 T. H. Ware, J. S. Biggins, A. F. Shick, M. Warner and T. J. White, *Nat. Commun.*, 2016, **7**, 10781.
22 A. Agrawal, A. C. Chipara, Y. Shamoo, P. K. Patra, B. J. Carey, P. M. Ajayan, W. G. Chapman and R. Verduzco, *Nat. Commun.*, 2013, **4**, 1739.
23 J. Küpfer and H. Finkelmann, *Macromol. Chem. Phys.*, 1994, **195**, 1353.
24 H. Wermter and H. Finkelmann, *e-Polym.*, 2001, **013**, 1.
25 A. Priimagi, C. J. Barrett and A. Shishido, *J. Mater. Chem. C*, 2014, **2**, 7155.
26 K. Sumioka, H. Kayashima and T. Tsutsui, *Adv. Mater.*, 2002, **14**, 1284.
27 G. Wu, Y. Jiang, D. Xu, H. Tang, X. Liang and G. Li, *Langmuir*, 2011, **27**, 1505.
28 H. Xing, J. Li, Y. Shi, J. Guo and J. Wei, *ACS Appl. Mater. Interfaces*, 2016, **8**, 9440.
29 Y. Jiang, D. Xu, X. Li, C. Lin, W. Li, Q. An, C. Tao, H. Tang and G. Li, *J. Mater. Chem.*, 2012, **22**, 11943.
30 Z. Yan, X. Ji, W. Wu, J. Wei and Y. Yu, *Macromol. Rapid Commun.*, 2012, **33**, 1362.
31 T. A. Singleton, I. B. Burgess, B. A. Nerger, A. Goulet-Hanssens, N. Koay, C. J. Barrett and J. Aizenberg, *Soft Matter*, 2014, **10**, 1325.
32 J. Zhao, Y. Liu and Y. Yu, *J. Mater. Chem. C*, 2014, **2**, 10262.
33 S. Kubo, Z.-Z. Gu, K. Takahashi, Y. Ohko, O. Sato and A. Fujishima, *J. Am. Chem. Soc.*, 2002, **124**, 10950.
34 M. Yamada, M. Kondo, J.-I. Mamiya, Y. Yu, M. Kinoshita, C. J. Barrett and T. Ikeda, *Angew. Chem., Int. Ed.*, 2008, **47**, 4986.
35 M. Yamada, M. Kondo, R. Miyasato, J. Mamiya, M. Kinoshita, Y. Yu, C. J. Barrett and T. Ikeda, *Mol. Cryst. Liq. Cryst.*, 2009, **498**, 65.
36 R. Tatsumi, J.-I. Mamiya, M. Kinoshita and A. Shishido, *Sci. Adv. Mater.*, 2014, **6**, 1432.
37 N. Akamatsu, M. Aizawa, R. Tatsumi, K. Hisano, A. Priimagi and A. Shishido, *J. Photopolym. Sci. Technol.*, 2016, **29**, 145.
38 Y. Naka, J.-I. Mamiya, A. Shishido, M. Washio and T. Ikeda, *J. Mater. Chem.*, 2011, **21**, 1681.
39 M. Yamada, M. Kondo, R. Miyasato, Y. Naka, J.-I. Mamiya, M. Kinoshita, A. Shishido, Y. Yu, C. J. Barrett and T. Ikeda, *J. Mater. Chem.*, 2009, **19**, 60.